Oblique evanescent excitation of a dielectric strip:
A model resonator with an open optical cavity of unlimited Q

Manfred Hammer*, Lena Ebers, and Jens Förstner

Theoretical Electrical Engineering, Paderborn University, Paderborn, Germany

Abstract: A rectangular dielectric strip at some distance above an optical slab waveguide is being considered, for evanescent excitation of the strip through the semi-guided waves supported by the slab, at specific oblique angles. The 2.5-D configuration shows resonant transmission properties with respect to variations of the angle of incidence, or of the excitation frequency, respectively. The strength of the interaction can be controlled by the gap between strip and slab. For increasing distance, our simulations predict resonant states with unit extremal reflectance of an angular or spectral width that tends to zero, i.e. resonances with a Q-factor that tends to infinity, while the resonance position approaches the level of the guided mode of the strip. This exceptionally simple system realizes what might be termed a "bound state coupled to the continuum".

Keywords: photonics, integrated optics, dielectric resonators, rectangular cavities, strip waveguides, oblique excitation, ultra-high quality factor, bound state coupled to the continuum.

1 Introduction

Dielectric optical cavities, if based either on total internal reflection, or on finite-sized periodically corrugated regions (photonic crystals), are always deemed to be inherently lossy [1]. Even in a limit of weak excitation, these inherent losses establish an upper bound to their quality factors (Q-factors). Among the variety of concepts, we look specifically at dielectric cavities of rectangular shape, such as the resonator device outlined in Fig. 1(b). If considered in a standard 2-D setting, specific dimensioning is required to obtain resonator elements of tolerable quality [2–4]. We shall reason in this paper, however, that the — rather arbitrarily rectangularly shaped — cavity of Fig. 1 supports in fact resonant states of in principle *infinite* Q (the lossless guided modes of the dielectric strip, accepting standard idealized theoretical models). The arguments require merely a change in excitation conditions: As illustrated in Fig. 1(a), we reconsider the resonator device in a "2.5-D" setting, with excitation of the strip by vertically (x-) guided, laterally (y, z-) nonlocalized waves at oblique angles of incidence θ.
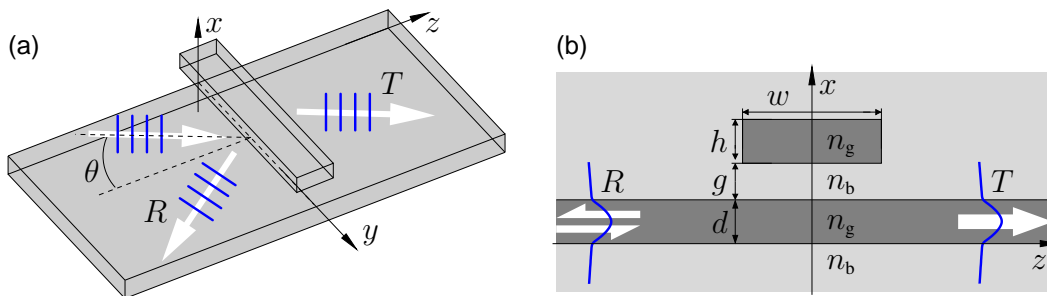

Figure 1: Oblique evanescent excitation of a dielectric strip, schematic (a), and cross section view (b). Cartesian coordinates x, y, z are oriented such that x is normal to the slab plane, while y is parallel to the strip axis. The incoming semi-guided wave propagates in the y-z-plane at an angle θ with respect to the strip normal. Outgoing waves with reflectance R and transmittance T are observed under the same angle. Parameters: refractive indices $n_g = 3.45$ (guiding regions), $n_b = 1.45$ (substrate, gap layer, and cladding), slab thicknesses $d = h = 0.22\,\mu m$, strip width $w = 0.5\,\mu m$, variable gap g. TE excitation around a vacuum wavelength $\lambda = 1.55\,\mu m$ is considered.

Similar configurations have been investigated previously, partly for other purposes. Among the earlier proposals are concepts for interferometers based on semi-guided waves passing a multimode rib segment at normal

---

* *Paderborn University, FG Theoretical Electrical Engineering*   *Warburger Straße 100, 33098 Paderborn, Germany*
Phone: ++49(0)5251/60-3560   Fax: ++49(0)5251/60-3524   E-mail: manfred.hammer@uni-paderborn.de

incidence, for application as polarizers [5] or isolators [6], a setting for the observation of lateral whispering gallery resonances at angled crossings of optical fibers [7], and, quite recently, a setup for the differentiation and integration of semi-guided beams [8], and for the observation of high-Q resonances [9]. Those latter studies consider the structure of Fig. 1 in a rib-waveguide form ($g = 0$), i.e. with the strip resting directly on the substrate. For more general notions on "oblique semi-guided waves", and for other device concepts, we refer to papers [10–14], where a recent overview [15] includes already a preliminary glimpse of the present results.

2   Oblique evanescent excitation of a dielectric strip

A dielectric strip of — within limits — arbitrary width and height is placed at some distance on top of a slab waveguide. The strip constitutes the cavity that is excited, here potentially at oblique angles, by the semi-guided waves in the slab, which thus works as our bus waveguide. The parameters given in the caption of Fig. 1 represent values for silicon slab and strip cores in a SiO_2 background medium, at a typical infrared wavelength.

This concerns time harmonic fields $\sim \exp(i\omega t)$ at angular frequency $\omega = kc = 2\pi c/\lambda$, for vacuum wavelength λ, wavenumber k, and speed of light c. Referring to Fig. 1, we consider a semi-guided incoming wave at angle θ with a functional dependence $\sim \mathbf{\Psi}(k_y, x) \exp(-i(k_y y + k_z z))$. The wave is based on the fundamental guided TE mode of the slab, with profile $\mathbf{\Psi}$ and effective mode index N_{TE0}, propagating with in-plane wavenumbers $k_y = kN_{TE0}\sin\theta$ and k_z, such that $k^2 N_{TE0}^2 = k_y^2 + k_z^2$ holds. Our entire problem is homogeneous along y. Hence the global solution of the frequency-domain Maxwell equations can be restricted to the single spatial Fourier component k_y as given by the incident wave, or the angle of incidence θ, respectively.

In particular, also any outgoing, guided- as well as nonguided waves share this specific y dependence. Following the fairly general reasoning of [13, 15], we consider some particular outgoing wave in modal form, similar to the incoming wave, with a potentially different effective index N_{out}, scattered in a direction ζ. That wave is then characterized by wavenumbers k_y and k_ζ that satisfy the relation $k^2 N_{out}^2 = k_y^2 + k_\zeta^2 = k^2 N_{TE0}^2 \sin^2\theta + k_\zeta^2$. Depending on the relative magnitude of the effective indices involved, and on the angle of incidence, that particular outgoing wave is either a propagating mode, or, for $k_\zeta^2 < 0$, it becomes evanescent. In the latter case the wave does not carry any power away from the region around the strip discontinuity.

Observing that all nonguided, radiative modal fields associated with the structure of Fig. 1 are characterized by effective mode indices below the limit of the background refractive index n_b, one can thus identify a critical angle θ_b with $\sin\theta_b = n_b/N_{TE0}$, such that, for $\theta > \theta_b$, all these waves become evanescent. Consequently, all radiation losses are suppressed for excitation of our strip at angles beyond θ_b. Likewise, the guided TM mode supported by the slab, with effective index N_{TM0}, can be associated with a critical angle θ_{TM} with $\sin\theta_{TM} = N_{TM0}/N_{TE0}$. Hence, for excitation at angles $\theta > \theta_{TM} > \theta_b$, also any power transfer to outgoing semi-guided TM waves is prohibited. In that regime, the reflectance and transmittance values for the fundamental TE slab mode strictly add up to one.

3   Solvers

These problems are governed by the Maxwell equations in the frequency domain. For the strictly y-harmonic incident fields, these can be reduced to a system of two coupled second order equations, for two principal field components, parameterized by the given wavenumber k_y. These equations are to be solved on a 2-D computational domain that covers the strip region, with transparent boundary conditions that can accommodate the incoming fields. In fact the expressions are formally equal to the standard equations that govern the modes of dielectric waveguides with 2-D cross sections [16]. In our case, however, these are to be treated as a scattering problem, not as an eigenvalue system; the given wavenumber k_y replaces the propagation constant (eigenvalue).

The results discussed below are generated with two types of numerical techniques. A quasi-analytical solver, based on a rigorous vectorial expansion into 1-D eigenmodes along both of the cross section coordinates (vectorial quadridirectional eigenmode expansion, vQUEP, [11, 17, 18]) appears to be robust, accurate, and comparably efficient for the present problems. Alternatively, the finite-element (FE) solvers included in the COMSOL multiphysics suite [19] cover these parameterized 2-D problems as well. Our results on structures with rounded

edges in [14, 20] are based on those tools; for the following examples, the COMSOL suite has been used for the successful corroboration of the vQUEP results.

Failure of both (probably of any) solvers for large gap distances is to be expected. According to our findings with the present numerical experiments, we attribute this to two related reasons. On the one hand, the overall field can be viewed roughly as consisting of two components, the field located around the strip core, and the waves confined to the slab, including the incoming wave. These interact (are "coupled") by increasingly lower levels, relative to the field maximum of the component, of the exponential tails of both fields at the position of the respective other component. Obviously, at a distance where — if not in an idealized theoretical, mathematical sense, but for all practical and numerical purposes — the interaction ceases to exist, the amplitude of the strip mode is no longer determined by the incoming wave in the slab. For such a configuration, any numerical scheme must eventually lead to an inhomogeneous system of linear equations (with the initially unknown parts of the optical field represented by the unknowns, and the right hand side given by the known incoming field) with a system matrix that is singular, i.e. does not have a unique solution. At smaller separations, for still interacting components, the system will gradually slide into the "singular" regime, with exceedingly ill-conditioned system matrices for growing gap g.

On the other hand, for increasing gaps, the solutions show increasingly stronger field amplitudes in the strip region, with the field shape there tending towards the guided mode of the strip. Note that this concerns the hybrid, vectorial TE-like fundamental mode of the rectangular strip, with potentially diverging fields [21] at the strip edges. Assuming that, for some given numerical setting, this strip mode is being approximated with limited accuracy only, errors introduced in this way must be expected, with growing relative strength, to influence the accuracy of the overall solution. With both solvers we observed an increasing violation of the overall power balance, in particular for close-to-resonant configurations, when increasing the gap g. To some degree, this can be compensated by adjusting the computational parameters, i.e. by increasing the spectral density of the modal basis in case of the vQUEP solver, or by reducing the finite element mesh size for the COMSOL simulations. For the data as shown, computational parameters have been selected (and have been readjusted over the series of computations, where necessary) such that, for normalized input, the total outgoing power does not deviate by more than 2% from unity.

4 Resonator characteristics

Our analysis starts with computing the guided mode of the dielectric strip. For the parameters as given in the caption of Fig. 1, at a vacuum wavelength of $\lambda = \lambda_m = 1.55\,\mu$m, COMSOL predicts a fundamental guided TE-like hybrid mode with effective index $N_m = 2.4192$ (further modes are supported). In line with the discussion of Section 2, this can be translated to an angle of incidence θ_m with $kN_m = kN_{TE0}\sin\theta_m$ of $\theta_m = 58.99°$, where the propagation constant kN_m of the strip mode matches the wavenumber k_y of the incident wave. We can thus expect to find a resonance, if the strip is excited at angles close to θ_m. Figure 2(a) shows a respective sweep over θ; the panels of Fig. 3 illustrate some corresponding fields.
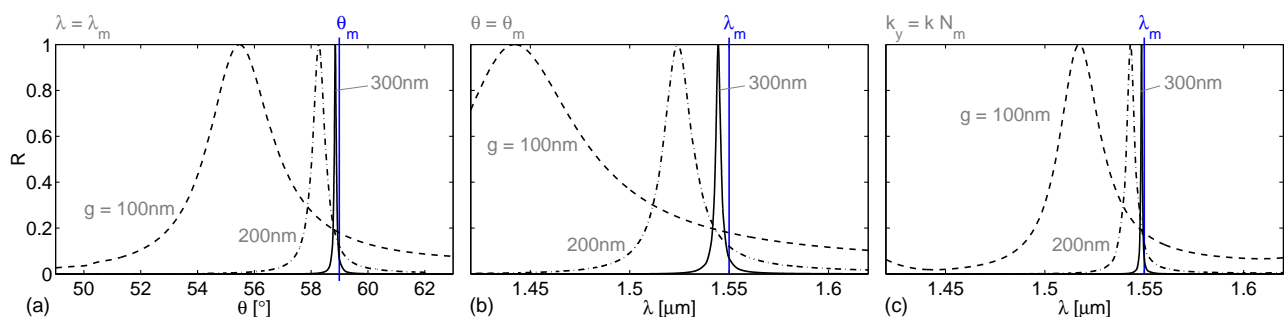

Figure 2: *Transmission properties of the strip-resonator of Fig. 1, for gaps $g = 100\,nm$ (dashed line), $g = 200\,nm$ (dash-dotted), and $g = 300\,nm$ (solid curve). The panels show the reflectance R as a function of the angle of incidence θ, for fixed vacuum wavelength λ (a), or as a function of the vacuum wavelength λ, for fixed angle of incidence (b), and for fixed wavenumber k_y (c).*
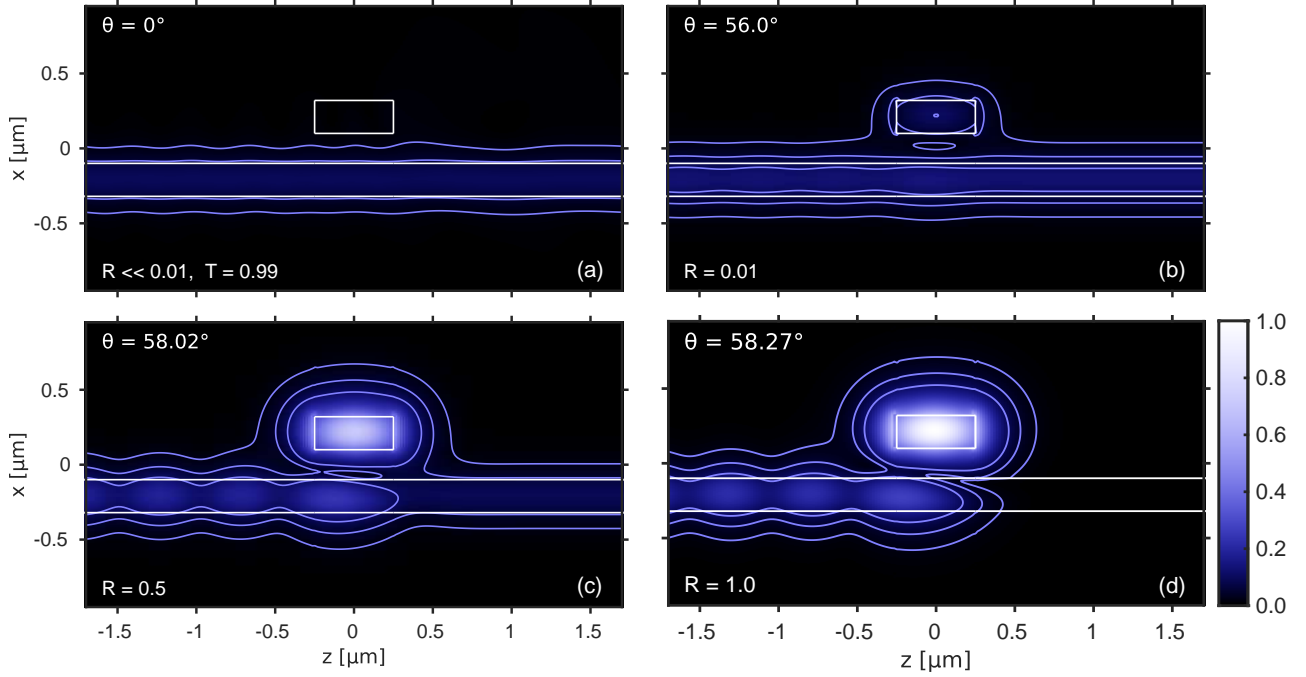
Figure 3: Absolute electric field strength $|\boldsymbol{E}|$ on the x-z-cross section plane, for the dielectric strip resonator of Fig. 1 with a gap of $g = 200\,\text{nm}$, at angles of incidence $\theta = 0°$ (a, normal incidence), $\theta = 56°$ (b, still off resonance), $\theta = 58.02°$ (c, at "half maximum" of the resonance), and $\theta = 58.27°$ (d, at resonance). The color levels of the panels are comparable; the contours indicate the levels of 2%, 5%, and 10% of the overall field maximum.

At normal incidence, shown in Fig. 3(a), the incoming wave just passes by underneath the strip, with only minor disturbance: Even if the incident TE slab mode is phase-matched with the TE slab mode in the strip (slab and strip are of the same thickness), the width w of the strip is much shorter than the coupling length associated with the symmetric double-core slab system (a half-beat length of $6.84\,\mu\text{m}$, for $g = 200\,\text{nm}$). Radiative losses are present, but remain negligible. Excitation at angles closer to θ_m leads to stronger fields in the region around the strip (plots Fig. 3(b), still "off resonance", Fig. 3(c), at half resonance, and Fig. 3(d), at resonance). The field shape there resembles more and more the fundamental TE-like guided mode of the strip. Reflectance levels raise to a maximum of $R = 100\%$ at resonance in Fig. 3(d), where consequently no transmitted waves can be seen in the slab region. Note that, due to the presence of the slab, the maximum reflectance is reached at an angle that differs from θ_m. For the parameters of Fig. 1, the critical angles, as introduced in Section 2, are $\theta_\text{b} = 30.9°$ and $\theta_\text{TM} = 46.3°$. Therefore, with the exception of Fig. 3(a), radiation losses and scattering into guided TM fields are suppressed for all configurations of Figs. 2–4; TE reflectance and TE transmittance total to 100%.

When viewing the structure as a resonator configuration, it might appear more natural to adopt the vacuum wavelength as the tuning parameter. Our focus is on sharp resonances, hence we neglect material dispersion. Two slightly different settings are considered. On the one hand, with a view to actual experiments, the angle of incidence θ is set to the value of θ_m. This implies, however, that the wavenumber $k_y = kN_\text{TE0}\sin\theta$ changes, due to the wavelength dependence of the vacuum wavenumber k and of the effective index N_TE0. Both dependences are smooth (i.e. nonresonant) in the wavelength range that is relevant for the observation of the narrow resonances. Alternatively, as a perhaps theoretically more straightforward constraint, the wavenumber k_y is kept constant at the level kN_m of the propagation constant of the strip mode (this then requires to readjust the angle of incidence). Some respective wavelength scans are shown in Figs. 2(b) and 2(c).

Since the strip cavity itself does not show any radiation losses, the resonance characteristics are determined solely by the strength of the interaction with the bus waveguide. Resonances can thus be controlled by the gap distance g. Figure 4 summarizes resonance properties, extracted from scans as in Fig. 2, corresponding either to the fixed frequency view Fig. 4(a), or to the settings with constant angle or wavenumber Fig. 4(b). For increasing gap, the resonance angle θ_r tends to the value θ_m of the strip mode Fig. 4(a). This is accompanied by a narrowing angular width $\Delta\theta$ of the resonance. According to Fig. 4(b), equivalent features can be observed when varying the vacuum wavelength, for either constant angle of incidence, or constant wavenumber. In line

with the plots of Fig. 2, the "height" of the resonance peaks, the maximum reflectance at resonance, remains at unity. This has been observed for all configurations discussed in this paper.
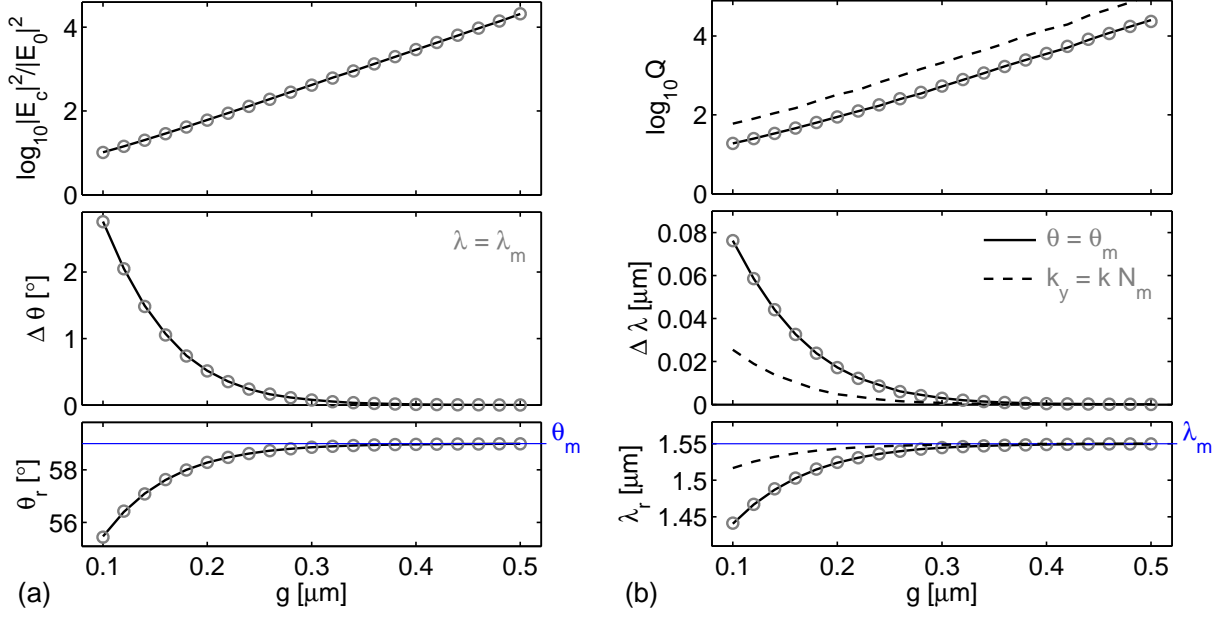

Figure 4: Resonance characteristics for the strip resonator of Fig. 1. Positions θ_r, λ_r of the resonances and full-widths-at-half-maxima $\Delta\theta_r$, $\Delta\lambda_r$ are shown as functions of the gap distance g, for angular scans with constant vacuum wavelength (a), and for wavelength scans with either constant angle of incidence $\theta = \theta_m$ (continuous lines & markers) or constant wavenumber $k_y = kN_m$ (dashed lines) (b). Uppermost logarithmic plots, (a): Absolute square of the electric field strength E_c at the center of the strip cavity, relative to the field strength E_0 at the center of the lower slab (for incoming TE mode at an angle of $59°$, at $\lambda = 1.55\,\mu m$), for absent strip. (b) Quality factor Q associated with the strip resonances. Lines: vQUEP results [11]; markers: FE-simulations (COMSOL [19]).

With a view to potential applications, the "field enhancement" properties of the structure might become relevant. According to Fig. 4(a), the ratio of the electric field strength at the center of the rib, at resonance, normalized to the field at the center of the slab, for absent strip, grows exponentially with the gap between the strip and the slab. While the plot corresponds to angular scans for fixed vacuum wavelength, matching curves (on the scale of the figure, not shown) are obtained in respective wavelength scans: At least in a regime of large g the respective resonant states correspond to a set of parameters $\lambda \approx \lambda_m$, $\theta \approx \theta_m$, $k_y \approx kN_m$, i.e. the corresponding fields coincide. Further, the upper panel of Fig. 4(b) shows the quality factor Q of the strip resonator [1], here evaluated as the ratio $Q = \lambda_r/\Delta\lambda_r$. Also in this case an exponential growth Q vs. g is observed. What concerns extremal levels for Q and the "field enhancement", we did not observe any limits in our numerical experiments. The data ranges as given are merely limited by how far we can trust our solvers (cf. the remarks in Section 3).

Finally we add brief thoughts on the formation of these resonances (roughly adhering to concepts from e.g. [22, 23]). To that end we adopt the point of view of the system with constant wavenumber $k_y = kN_m$. The following "states" can then be distinguished:

1. the isolated bound state, i.e. the guided TE-like mode supported by the strip, for absent slab (or, alternatively, in a limit of "large" g). This bound state is characterized by the real eigenfrequency $\omega_m = 2\pi c/\lambda_m$.

2. the incoming semi-guided plane waves supported by the slab, for absent strip. The slab supports a continuum of these waves in a range of frequencies around ω_m.

3. the eigenstate of the composite system of strip and slab, for finite g, and *for absent external excitation*. This would be an eigensolution characterized by an eigenfrequency that is complex owing to the leakage into the slab. Due to the symmetry of the problem, this state necessarily radiates with equal rate into the semi-guided TE-waves at angles $\approx \theta_m$ in *both* the positive and negative z-direction. At finite g the presence of the slab causes the real part of its eigenfrequency to deviate from ω_m ("coupling induced phase shifts" [24]). For increasing g the level of leakage, and consequently the relative field strength in the slab core, decreases; the composite state tends towards the former bound state (1).

4. the transmission states realized by the excitation of the composite system by the incoming semi-guided waves, for finite g, as calculated in our simulations. These can be thought of as superpositions of the unperturbed incoming semi-guided plane wave (2), and the former composite eigenstate (3), with relative weights that depend on the excitation wavelength. Off resonance, for growing g, this state separates into the bound state (1) (with increasingly less well defined amplitude) and the unpertubed normalized incoming wave (2).

Close to the resonance, this last superposition (4) leads to partly destructive interference of the waves associated with the states (2) and (3) in the slab region $z > 0$, i.e. leads to a diminished transmittance and increased reflectance. At resonance, along with the unit reflectance, complete destructive interference of states (2) and (3) is observed in the region "after" the strip.

Obviously, all extremal resonance properties rely essentially on the *infinite extent* of the incoming wave along the axis y of homogeneity of the structure. Incoming fields with limited lateral width, e.g. in the form of Gaussian wave packets [8, 13], or in the form of wave bundles adapted to a guided mode of a wide, weakly etched rib [14], necessarily contain semi-guided waves with some range of relevant k_y wavenumbers. The strip-resonators will then act as (extremely narrowband) filters, or beam dividers [8], respectively.

5   Concluding remarks

Accepting the setting with fixed y-wavenumber and variable vacuum wavelength / frequency, for a configuration with *large* distance g, this would be an explicitly simple way to realize a system with a bound state (the rib mode, nonradiating in the limit of infinite g), and a wave continuum (the waves supported by the slab) in a range of frequencies that cover the (real) eigenfrequency of the bound state. Respective features have attracted substantial attention elsewhere [25–28] in the more recent past. Note that, in the present context of photonics, those phenomena appear to be most frequently discussed in a framework of elaborately tailored periodic structures / of photonic crystals.

Among the many proposals, the structures of [9, 29] are perhaps closest to our present configurations. Systems of strip-loaded waveguides [29], and a ridge waveguide with oblique excitation by semi-guided waves [9], are investigated. In both cases the singular resonant states are identified by tuning the width of the strip/ridge to particular values, where the — elsewhere broader — resonances associated with the leaky modes of the waveguide shrink to zero angular width. The height of the resonances remains at unit reflectance. This is attributed to specific symmetry and phase properties of the waves that carry the directional leakage in the lateral slab.

What concerns our strip with oblique evanescent semi guided excitation, we just as well observe fully formed resonant states (both in the angular and spectral setting) of a width that tends to zero, if one tunes the gap distance g to the specific value of infinity. A symmetry argument does not apply, though; further, with a view to the "definition" of the special states from [26], one could doubt whether the (large) spatial separation of the bound strip mode and the continuum of semi-guided waves in the slab qualifies for a "coexistence" of states. Hence, here the notion of a "bound state coupled to the continuum" might perhaps be more adequate.

Funding

References

[1] I. Chremmos, O. Schwelb, and N. Uzunoglu, editors. *Photonic Microresonator Research and Applications*. Springer Series in Optical Sciences, Vol. 156. Springer, London, 2010.

[2] C. Manolatou, M. J. Khan, S. Fan, P. R. Villeneuve, H. A. Haus, and J. D. Joannopoulos. Coupling of modes analysis of resonant channel add-drop filters. *IEEE Journal of Quantum Electronics*, 35(9):1322–1331, 1999.

[3] M. Lohmeyer. Mode expansion modeling of rectangular integrated optical microresonators. *Optical and Quantum Electronics*, 34(5):541–557, 2002.

[4] M. Hammer. Resonant coupling of dielectric optical waveguides via rectangular microcavities: The coupled guided mode perspective. *Optics Communications*, 214(1–6):155–170, 2002.

[5] M. Lohmeyer and R. Stoffer. Integrated optical cross strip polarizer concept. *Optical and Quantum Electronics*, 33(4/5):413–431, 2001.

[6] M. Lohmeyer, L. Wilkens, O. Zhuromskyy, H. Dötsch, and P. Hertel. Integrated magnetooptic cross strip isolator. *Optics Communications*, 189(4–6):251–259, 2001.

[7] T. A. Birks, J. C. Knight, and T. E. Dimmick. High-resolution measurement of the fiber diameter variations using whispering gallery modes and no optical alignment. *IEEE Photonics Technology Letters*, 12(2):182–183, 2000.

[8] E. A. Bezus, L. L. Doskolovich, D. A. Bykov, and V. A. Soifer. Spatial integration and differentiation of optical beams in a slab waveguide by a dielectric ridge supporting high-Q resonances. *Optics Express*, 26(19):25156–25165, 2018.

[9] E. A. Bezus, D. A. Bykov, and L. L. Doskolovich. Bound states in the continuum and high-Q resonances supported by a dielectric ridge on a slab waveguide. *Photonics Research*, 6(11):1084–1093, 2018.

[10] F. Çivitci, M. Hammer, and H. J. W. M. Hoekstra. Semi-guided plane wave reflection by thin-film transitions for angled incidence. *Optical and Quantum Electronics*, 46(3):477–490, 2014.

[11] M. Hammer. Oblique incidence of semi-guided waves on rectangular slab waveguide discontinuities: A vectorial QUEP solver. *Optics Communications*, 338:447–456, 2015.

[12] M. Hammer, A. Hildebrandt, and J. Förstner. How planar optical waves can be made to climb dielectric steps. *Optics Letters*, 40(16):3711–3714, 2015.

[13] M. Hammer, A. Hildebrandt, and J. Förstner. Full resonant transmission of semi-guided planar waves through slab waveguide steps at oblique incidence. *Journal of Lightwave Technology*, 34(3):997–1005, 2016.

[14] L. Ebers, M. Hammer, and J. Förstner. Oblique incidence of semi-guided planar waves on slab waveguide steps: Effects of rounded edges. *Optics Express*, 26(14):18621–18632, 2018.

[15] M. Hammer, L. Ebers, A. Hildebrandt, S. Alhaddad, and J. Förstner. Oblique semi-guided waves: 2-D integrated photonics with negative effective permittivity. In *2018 IEEE 17th International Conference on Mathematical Methods in Electromagnetic Theory (MMET)*, pages 9–15, 2018.

[16] C. Vassallo. *Optical Waveguide Concepts*. Elsevier, Amsterdam, 1991.

[17] M. Hammer. Quadridirectional eigenmode expansion scheme for 2-D modeling of wave propagation in integrated optics. *Optics Communications*, 235(4–6):285–303, 2004.

[18] M. Hammer. METRIC — Mode expansion tools for 2D rectangular integrated optical circuits. http://metric.computational-photonics.eu/.

[19] Comsol Multiphysics GmbH, Göttingen, Germany; http://www.comsol.com.

[20] L. Ebers, M. Hammer, and J. Förstner. Spiral modes supported by circular dielectric tubes and tube segments. *Optical and Quantum Electronics*, 49(4):176, 2017.

[21] A. S. Sudbø. Why are accurate computations of mode fields in rectangular dielectric waveguides difficult? *Journal of Lightwave Technology*, 10(4):418–419, 1992.

[22] M. Maksimovic, M. Hammer, and E. van Groesen. Field representation for optical defect microcavities in multilayer structures using quasi-normal modes. *Optics Communications*, 281(6):1401–1411, 2008.

[23] M. Maksimovic, M. Hammer, and E. van Groesen. Coupled optical defect microcavities in 1D photonic crystals and quasi-normal modes. *Optical Engineering*, 47(11):114601 1–12, 2008.

[24] M. A. Popović, C. Manolatou, and M. R. Watts. Coupling-induced resonance frequency shifts in coupled dielectric multi-cavity filters. *Optics Express*, 14(3):1208–1222, 2006.

[25] D. C. Marinica, A. G. Borisov, and S. V. Shabanov. Bound states in the continuum in photonics. *Physical Review Letters*, 100(18):183902, 2008.

[26] C. W. Hsu, B. Zhen, A. D. Stone, J. D. Joannopoulos, and M. Soljačić. Bound states in the continuum. *Nature Reviews Materials*, 1:16048, 2016.

[27] L. Yuan and Y. Y. Lu. Bound states in the continuum on periodic structures: perturbation theory and robustness. *Optics Letters*, 42(21):4490–4493, 2017.

[28] L. Yuan and Y.-Y. Lu. Bound states in the continuum on periodic structures surrounded by strong resonances. *Physical Review A*, 97:043828, 2018.

[29] C.-L. Zou, J.-M. Cui, F.-W. Sun, X. Xiong, X.-B. Zou, Z.-F. Han, and G.-C. Guo. Guiding light through optical bound states in the continuum for ultrahigh-Q microresonators. *Laser & Photonics Reviews*, 9(1):114–119, 2014.